Behavioral/Systems/Cognitive

SIRT1 Promotes the Central Adaptive Response to Diet Restriction through Activation of the Dorsomedial and Lateral Nuclei of the Hypothalamus

Akiko Satoh,[1] Cynthia S. Brace,[1] Gal Ben-Josef,[5] Tim West,[2] David F. Wozniak,[3,4] David M. Holtzman,[1,2,4] Erik D. Herzog,[4,5] and Shin-ichiro Imai[1]

Departments of [1]Developmental Biology, [2]Neurology, and [3]Psychiatry and [4]Hope Center for Neurological Disorders, Washington University School of Medicine, St. Louis, Missouri 63110, and [5]Department of Biology, Washington University, St. Louis, Missouri 63130

Diet restriction retards aging and extends lifespan by triggering adaptive mechanisms that alter behavioral, physiological, and biochemical responses in mammals. Little is known about the molecular pathways evoking the corresponding central response. One factor that mediates the effects of diet restriction is the mammalian nicotinamide adenine dinucleotide (NAD)-dependent deacetylase SIRT1. Here we demonstrate that diet restriction significantly increases SIRT1 protein levels and induces neural activation in the dorsomedial and lateral hypothalamic nuclei. Increasing SIRT1 in the brain of transgenic (BRASTO) mice enhances neural activity specifically in these hypothalamic nuclei, maintains a higher range of body temperature, and promotes physical activity in response to different diet-restricting paradigms. These responses are all abrogated in *Sirt1*-deficient mice. SIRT1 upregulates expression of the orexin type 2 receptor specifically in these hypothalamic nuclei in response to diet-restricting conditions, augmenting response to ghrelin, a gut hormone whose levels increase in these conditions. Our results suggest that in the hypothalamus, SIRT1 functions as a key mediator of the central response to low nutritional availability, providing insight into the role of the hypothalamus in the regulation of metabolism and aging in mammals.

Introduction

Animals employ a variety of strategies to survive when food is limited, including adaptive mechanisms that alter their behavioral, physiological, and biochemical responses to low nutritional inputs. For example, it has been reported that animals reduce their physical activity during the initial stages of food deprivation, but increase it during the later stages (Wang et al., 2006). This increase in physical activity could be an adaptive response to search for food and to survive through such life-threatening conditions. In rodents, the increase in physical activity has also been observed in diet restriction (DR) (Yu et al., 1985; Ingram et al., 1987), the single, most reliable regimen known to retard aging and extend lifespan in a variety of organisms, including yeast (Lin et al., 2000), worms (Lakowski and Hekimi, 1998), flies (Chapman and Partridge, 1996), rodents (McCay et al., 1935; Weindruch and Walford, 1982), and primates (Colman et al., 2009). DR has also been known to delay the onset and slow the progression of many age-related diseases (Weindruch et al., 1986; Bronson and Lipman, 1991; Fontana et al., 2004; Colman et al., 2009). Whereas a number of hypotheses have been proposed to explain mechanisms for the physiological effects of DR (Masoro, 2005), recent evidence suggests that DR triggers highly coordinated adaptive responses that translate nutritional cues to alterations in fundamental cellular processes, thereby mediating a variety of physiological responses at a systemic level (Sinclair, 2005; Bishop and Guarente, 2007a).

Although little is known about the mechanisms of these adaptive responses to DR, the evolutionarily conserved Sir2 (silent information regulator 2) family of NAD-dependent deacetylases/ADP-ribosyltransferases, also called "sirtuins," has recently drawn much attention as a critical regulator that mediates physiological responses to DR (Sinclair, 2005; Bishop and Guarente, 2007a; Imai, 2009a). Sirtuins play a critical role in the regulation of aging and longevity in experimental model organisms, such as yeast, worms, and flies (Kaeberlein et al., 1999; Tissenbaum and Guarente, 2001; Rogina and Helfand, 2004). Sirtuins are also required for the DR-mediated lifespan extension in those organisms with certain genetic backgrounds (Lin et al., 2000; Anderson et al., 2003; Rogina and Helfand, 2004; Wang and Tissenbaum, 2006). In mammals, there are seven sirtuins, SIRT1 through SIRT7. Numerous studies have demonstrated that SIRT1 regulates essential metabolic pathways in response to low energy intake in multiple tissues, as well as cell survival in response to stress and damage (Sinclair, 2005; Imai and Guarente, 2007; Schwer

Received March 17, 2010; revised June 10, 2010; accepted June 17, 2010.

This work was supported by the National Institute on Aging (AG02150), the Ellison Medical Foundation, and the Longer Life Foundation to S.I. A.S. is supported by Japan Society for the Promotion of Science Postdoctoral Fellowships for Research Abroad. S.I. serves as a scientific advisory board member for Sirtris, a GSK company. We thank Daniel Granados-Fuentes, Tatsiana Simon, and Sara Conyers for help with mouse behavioral tests, Christian Beaule for help with cFOS staining, Elise Oster for cloning of the mouse *Ox2r* promoter, and members of the Imai laboratory for their help and discussions.

Correspondence should be addressed to Dr. Shin-ichiro Imai, Department of Developmental Biology, Washington University School of Medicine, Campus Box 8103, 660 South Euclid Avenue, St. Louis, MO 63110. E-mail: imaishin@wustl.edu.

DOI:10.1523/JNEUROSCI.1385-10.2010

 0270-6474/10/3010220-13$15.00/0

and Verdin, 2008). Results from loss- and gain-of-function mouse studies have provided genetic evidence connecting SIRT1 to DR (Imai, 2009a). For example, it has been reported that the DR-induced elevation of physical activity is abrogated in *Sirt1*-deficient mice (Chen et al., 2005), providing a clue for the potential role of SIRT1 in the central regulation of physiological response to DR. Therefore, we decided to examine whether and how SIRT1 controls central adaptive responses to DR using both gain- and loss-of-function SIRT1 mutant mice. Our present study reveals a novel function for SIRT1 in the hypothalamus, particularly in the dorsomedial and lateral hypothalamic nuclei, as a key mediator of the central adaptive response to DR. These findings also provide important insight into the physiological mechanism that conveys the anti-aging and the lifespan-extending effects of DR in mammals.

Materials and Methods

BRASTO and Sirt1-deficient mice. To generate brain-specific SIRT1-overexpressing (BRASTO) transgenic mice, the mouse prion (PrP) promoter-driven, HA-tagged *Sirt1* transgene was constructed by inserting a 2.3 kb fragment of the mouse *Sirt1* cDNA into the vector carrying the mouse PrP promoter (Wang et al., 2005) (a kind gift from Dr. David Borchelt, University of Florida, Gainesville, FL) after eliminating three NotI sites without changing the SIRT1 amino acid sequence and adding the HA tag to the 3′ end of the *Sirt1* coding sequence. The PrP-*Sirt1*-HA transgene was linearized, purified, and microinjected into C57BL/6J × CBA hybrid blastocysts in the Washington University Mouse Genetic Core Facility. Transgenic mice were identified by PCR genotyping with tail DNA. Two transgenic founders (lines 1 and 10) were established, and the mice were backcrossed to wild-type C57BL/6 mice (Jackson Laboratories) for 6–7 generations before analysis. Nontransgenic littermates were used as controls. *Sirt1*-deficient (*Sirt1*$^{-/-}$) mice, which were originally established in the 129sv/B6 mixed background, were described previously (Cheng et al., 2003). *Sirt1*-heterozygous mice were backcrossed to wild-type FVB mice (Jackson Laboratories) for six generations (a kind gift from Dr. Jeffrey Milbrandt, Washington University, St. Louis, MO), and *Sirt1*$^{-/-}$ mice were generated by crossing *Sirt1*-heterozygous mice. *Sirt1*$^{-/-}$ FVB mice at 3–5 months of age were used for this study.

Diet-restricting paradigms. For 48 h fasting, chow was removed from both male and female mice at 4–5 months of age at 8:30 A.M. for 48 h. After 48 h fasting, the ambulatory behavior of mice was carefully recorded by a video camera, and physical activity was scored by counting the number of times that each mouse crossed from one quadrant to another over 10 min (supplemental Movies S1–4, available at www.jneurosci.org as supplemental material). For DR, wild-type C57BL/6, BRASTO, *Sirt1*$^{-/-}$, and respective control male mice at 8–12 weeks of age were fed with 1 g pellets of a semisynthetic chow, AIN-93M (Bioserv). *Ad libitum*-fed (AL) control mice were given pellets equal to calculated average daily food intake (~4 pellets), while diet-restricted mice were given pellets equal to 60% of average daily food intake. For short-term DR (14 d), mice were fed everyday at 5:00 P.M. and killed between 9:00 A.M. and 10:00 A.M. To assess the effects of this short-term DR on locomotor activity, the groups were tested over a 24 h (12 h/12 h light/dark) period according to previously published procedures (Wozniak et al., 2004). For long-term DR (104 d), the feeding cycle was as follows: 8 and 4–5 pellets on Monday and Wednesday and 10–11 and 6–7 pellets on Friday for AL and DR mice, respectively, and chow was delivered between 4:00 and 5:00 P.M. This DR regimen with intermittent feeding is to create conditions that allow us to conduct other physiological tests, such as intraperitoneal glucose tolerance tests, as similar as possible to regular procedures. In one of these DR experiments, for example, after 3 months of DR, glucose levels on Thursday morning were 150 ± 6.9 and 105 ± 4.5 mg/dl for AL and DR males, respectively, while glucose levels on Friday morning were 130 ± 6.0 and 76.4 ± 6.1 mg/dl for AL and DR males, respectively. Therefore, physiological tests that normally require fasting before the experiments were usually conducted on Wednesday or Friday morning, and we confirmed that DR mice showed significantly improved glucose tolerance (data not shown). However, to separate the long-term effects of DR from those of fasting, tissue and plasma samples were collected between 9:00 A.M. and 10:00 A.M. on Tuesday and Thursday morning. For timed DR, male mice at 4–5 months of age were maintained in 12 h/12 h light/dark schedule and housed individually with a running wheel. Mice were fed only from 1:00 P.M. [zeitgeber time 6 (ZT6)] to 5:00 P.M. (ZT10). Running-wheel revolutions in 1 min bins were recorded using Clocklab software (Actimetrics) as described previously (Aton et al., 2004). All animal procedures were approved by the Washington University Animal Studies Committee.

Twenty-four-hour locomotor activity test. Starting at 10:00–10:30 A.M., locomotor activity was evaluated over a 24 h period by placing individual mice into transparent (47.6 × 25.4 × 20.6 cm high) polystyrene enclosures as described in previous studies involving a 1 h test (Wozniak et al., 2004). Each enclosure was surrounded by a frame containing a 4 × 8 matrix of photocell pairs, the output of which was fed to an on-line computer (Hamilton-Kinder). Another frame that contained eight pairs of photocells and was raised 7 cm above the floor of the enclosure was used to quantify vertical activity. Variables that were analyzed included the total number of ambulations (whole-body movements), as well as the number of vertical rearings over the 24 h period.

Rectal body temperature. Rectal body temperature was measured at 9:00–9:30 A.M. by a Microtherma 2 Type (TW2-193) thermometer with a mouse rectal probe (model RET-3).

Immunohistochemistry. Mice were anesthetized with ketamine/xylazine and perfused with PBS followed by 4% paraformaldehyde (PFA). Brains were fixed with 4% PFA overnight and placed into 15% sucrose followed by 30% sucrose. Thirty-micrometer sections were made by a cryostat and stored at −30°C. Immunostaining results were analyzed for each hypothalamic nucleus as follows: Because brain sections from one mouse were used for multiple analyses, hypothalamic sections at the same coronal planes were always chosen for all mice analyzed. For each mouse, two brain sections around bregma −0.82 mm were used for the PVN and SCN and one to two brain sections around bregma −1.58 mm were used to cover the Arc, VMH, DMH, and LH. We usually used three to four mice for each analysis and therefore analyzed four to eight sections per hypothalamic nucleus. When signals/counts were relatively low, we analyzed more sections. To quantify SIRT1 protein signals in each hypothalamic nucleus, brain sections were stained by 3,3′-diaminobenzidine (DAB) with rabbit anti-mouse SIRT1 (1:3000) (Moynihan et al., 2005) and biotinylated goat anti-rabbit IgG (1:500) antibodies with the ABC kit (Vector Laboratories). SIRT1 protein signals were quantified by measuring the intensity per area in each hypothalamic nucleus after subtracting surrounding background signal levels using the Histogram function of Adobe Photoshop. For double immunofluorescent staining of HA-tagged SIRT1, samples were stained first with the same rabbit anti-mouse SIRT1 (1:1000) and HRP-conjugated goat anti-rabbit IgG (1:2000) antibodies using the FITC TSA kit (Parkin Elmer) and then with anti-HA (1:1000, Covance) and HRP-conjugated goat anti-mouse IgG (1:10,000) antibodies using the Cy3 TSA kit, according to the manufacturer's protocol. To stain cFOS in each hypothalamic nucleus, samples were stained by the DAB detection method with anti-cFOS (1:100,000, Calbiochem) and biotinylated goat anti-rabbit IgG (1:200) antibodies with the ABC kit. The numbers of cFOS-positive cells were quantified by ImageJ software. For the double staining of cFOS and OX2R, samples were stained for cFOS first and then with anti-OX2R (1:100, Alpha Diagnostics) and HRP-conjugated goat anti-rabbit IgG (1:1000) antibodies with the Cy3 TSA kit.

In situ *hybridization.* Brain sections were fixed in 4% PFA, acetylated with triethanol amine/acetic anhydrite, and prehybridized in hybridization buffer (10 mM Tris-HCl [pH 7.4], 600 mM NaCl, 1 mM EDTA, 1× Denhardt's solution, 25 μg/ml yeast ribosomal RNA, 12.5 μg/ml salmon testis DNA, 10% dextran sulfate, and 40% formamide). Prehybridized samples were then hybridized in hybridization buffer containing digoxigenin (DIG)-labeled antisense RNA probes of *Ox2r* (nucleotides 595-1034) at 60°C overnight. Sense probes were used as negative controls. After samples were hybridized, samples were sequentially washed with 2× SSC/50% formamide, 0.1× SSC, and washing buffer (100 mM maleic acid, 150 mM NaCl, 0.3% Tween 20, pH 7.5) and then incubated with

blocking solution (PerkinElmer). Signals were visualized by incubating with a peroxidase-conjugated anti-DIG antibody and the TSA kit. The signal intensity per area in each hypothalamic nucleus was quantified after subtracting surrounding background signal levels by using the Histogram function of Adobe Photoshop.

Laser-microdissection. The brain was removed, immediately frozen in OCT compound on dry ice, and stored at −80°C until laser-microdissection. Twenty-five-micrometer brain sections were mounted on PEN-membrane slides (Leica), and kept on dry ice. The mounted slides were hydrated sequentially in 100%, 95%, 75%, and 50% ethanol for 30 s each. The hydrated slides were stained with 1% Cresyl Violet (Sigma) for 1 min, and dehydrated with 50%, 75%, 95%, and 2 cycles of 100% ethanol for 30 s each. The dehydrated slides were then incubated in xylene twice for 1 min each. After being air-dried for 5 min, Arc, VMH, DMH, and LH were microdissected using the Leica LMD 6000 laser-microdissection system.

Quantitative real-time RT-PCR. Total RNA was extracted from each hypothalamic nucleus using the RNeasy kit (Qiagen) and reverse-transcribed into cDNA with the High Capacity cDNA Reverse Transcription kit (Applied Biosystems). Quantitative real-time RT-PCR was conducted with the TaqMan Fast Universal PCR Master mix and appropriate TaqMan primers for each gene in the GeneAmp 7500 fast sequence detection system (Applied Biosystems). Relative expression levels were calculated for each gene by normalizing to *Gapdh* levels and then to one of the wild-type control individuals.

Luciferase assay. HEK293 cells were transfected with a luciferase reporter driven by a ~1 kb *Ox2r* promoter and a *Sirt1* minigene or a control vector (Revollo et al., 2004). Transfected cells were cultured in media with 5 mM glucose for 48 h. Cell extracts were prepared, and luciferase activity was determined with the Dual-Luciferase Reporter Assay System (Promega) according to the manufacturer's protocol. Luciferase activity levels were normalized to protein concentrations of each sample.

Chromatin-immunoprecipitation assay. Mouse hypothalamus was incubated sequentially with freshly prepared 5 mM DTBP and 1% PFA. After washing with PBS, pellets were stored at −80°C until analysis. Pellets were resuspended in buffer (1% Triton X-100, 0.1% deoxycholate, 50 mM Tris-HCl [pH 8.1], 5 mM EDTA, 150 mM NaCl, 1% SDS, and protease inhibitors) and placed on ice for 20 min. After centrifugation, chromatin was sheared by sonicating with nuclei buffer (50 mM Tris-HCl, pH 8.0, 10 mM EDTA, 0.01% SDS, and 0.1 mM PMSF) to a final size between 200 bp and 600 bp. Before immunoprecipitation, soluble chromatin was incubated with protein A agarose/salmon slurry (Millipore) at 4°C for 30 min. An aliquot of supernatant was removed as "input" and used in PCR analysis. The remainder of supernatant was incubated with SIRT1 antibody or rabbit IgG at 4°C overnight. Immune complexes were isolated by incubating with protein A agarose/salmon slurry for 1.5 h at 4°C. The complexes were washed with low-salt buffer, high-salt buffer, LiCl buffer, and TE, pH 8.0. The complexes were eluted, de-cross-linked with 125 mM NaCl at 65°C overnight, and then treated with RNase A at 37°C for 30 min and with proteinase K at 45°C for 90 min. The purified DNA was resuspended with TE and analyzed by PCR by specific primer sets.

Measurement of serum ghrelin levels. Mouse plasma samples were collected into tubes containing 4-(2-aminoethyl)-benzenesulfonyl fluoride (AEBSF, Sigma), incubated for 30 min at room temperature, and centrifuged at 5000 × *g* for 10 min at 4°C. The supernatant was stored at −30°C until analysis. The levels of ghrelin in serum were determined by a rat/mouse total ghrelin ELISA kit (LINCO Research).

Ghrelin administration. After 4 d of habituation to handling and mock injection, BRASTO, *Sirt1*$^{-/-}$, and control male mice were injected with octanoylated rat ghrelin (Pi Proteomics) at a dose of 30 nmol/kg body weight or with an equal volume of PBS. Ninety and one hundred twenty minutes after injection, mice were anesthetized and killed to collect brains.

Statistical analyses. Statistical analyses were performed using unpaired or paired Student's *t* tests for two groups and one-way ANOVA with the Tukey–Kramer *post hoc* test for more than two groups. Two-way ANOVA was also applied to the data shown in Figures 2*A*, 3*D*, 3*E*, 4*A*, 4*D*, 4*E*, 7*A*, and 7*C*, to assess the main effects of two different factors and the interaction between them. For this analysis, full statistics are presented in supplemental Table S1 (available at www.jneurosci.org as supplemental material). A Wilcoxon matched-pairs signed-ranks test was used to compare differences of hourly wheel counts through the light and dark times between wild-type versus BRASTO mice and day 0 vs day 5 in each genotype, respectively. In all analyses, we set the α level at 0.05. We used Microsoft Excel 2008 and SPSS 11.0 to conduct statistical analyses.

Results

SIRT1 is expressed in major hypothalamic nuclei

We initially surveyed the expression pattern of the SIRT1 protein in the mouse brain using a rabbit polyclonal, affinity-purified antibody (Imai et al., 2000). This antibody did not produce any significant positive signals on *Sirt1*-deficient brain sections, assuring its specificity (supplemental Fig. S1*A*,*B*, available at www.jneurosci.org as supplemental material). SIRT1 showed nuclear localization in the hypothalamus and hippocampus, and extranuclear localization in dorsal regions of the cerebral cortex (data not shown). In the hypothalamus, SIRT1 was expressed in the arcuate nucleus (Arc), the ventromedial, dorsomedial, and lateral hypothalamic nuclei (VMH, DMH, and LH, respectively), and the paraventricular nucleus (PVN), brain regions that all play critical roles in the central regulation of adaptive responses to food availability (Elmquist, 2001) (Fig. 1*A*). SIRT1 was also expressed in the suprachiasmatic nucleus (SCN), a region important for the central regulation of circadian rhythm (Green et al., 2008) (Fig. 1*A*). These results are consistent with the reported distribution of *Sirt1* mRNA in the hypothalamus (Ramadori et al., 2008).

Both SIRT1 levels and the number of activated neurons increase in the DMH and LH of diet-restricted hypothalami

Because SIRT1 protein levels are upregulated and downregulated in multiple tissues and even within the same tissue in response to DR (Imai and Guarente, 2007; Chen et al., 2008; Schwer and Verdin, 2008), we decided to examine whether SIRT1 protein levels were also altered in hypothalamic nuclei of diet-restricted mice. Using a semiquantitative DAB-based immunostaining method with our highly specific SIRT1 antibody (supplemental Fig. S1*A*,*B*, available at www.jneurosci.org as supplemental material), we found that SIRT1 protein levels moderately but specifically increased in the DMH, LH, and SCN, but not in the Arc, VMH, or PVN, in response to short-term (14 d) DR (DMH, $p = 0.047$; LH, $p = 0.043$; SCN, $p = 0.007$) (Fig. 1*B*; supplemental Fig. S2, available at www.jneurosci.org as supplemental material). We also observed significant increases in the number of cFOS-positive cells, a well established marker of neural activation (Sagar et al., 1988; Dragunow and Faull, 1989), in the DMH and LH under DR (DMH, $p = 0.019$; LH, $p < 0.001$) (Fig. 1*C*,*D*). Neither the hippocampus nor the cortex showed any significant increase in cFOS-positive cells (data not shown). Similar results were obtained in hypothalami under long-term (104 d) DR (supplemental Fig. S3*A*–*D*, available at www.jneurosci.org as supplemental material). These findings suggest that a moderate but continuous increase in SIRT1 dosage and/or activity might play an important role in neural activation in the DMH and LH in response to DR.

To address this possibility, we generated transgenic mice in which SIRT1 protein levels are selectively increased in the brain (BRASTO). BRASTO transgenic mice express a C-terminally HA-tagged mouse SIRT1 cDNA driven by the mouse prion promoter (Fig. 1*E*). We established two independent BRASTO transgenic lines, lines 1 and 10. Both lines showed moderate in-

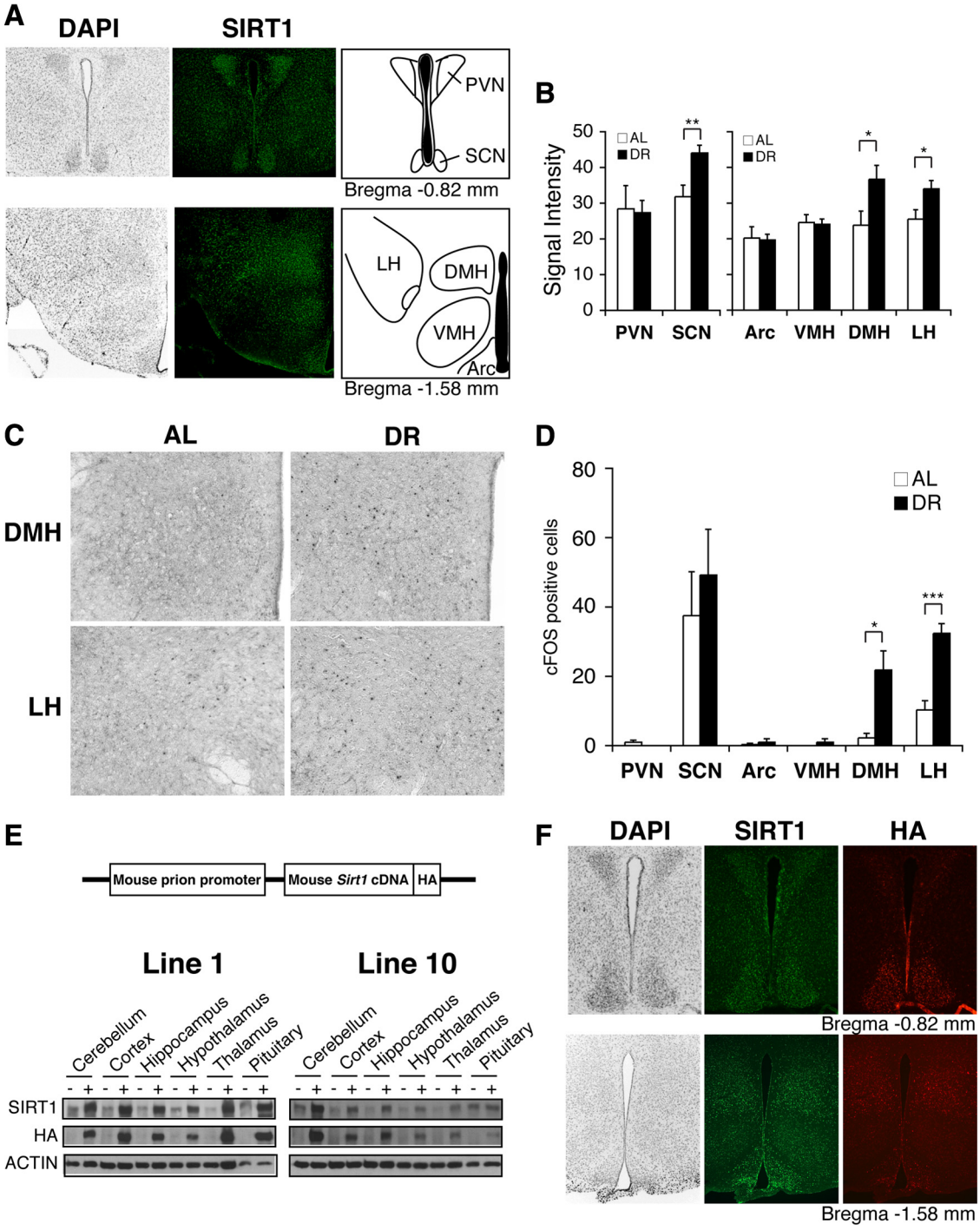

Figure 1. SIRT1 is expressed in major hypothalamic nuclei, and both SIRT1 levels and the number of activated neurons increase in the DMH and LH in diet-restricted hypothalami. ***A***, Immunofluorescent staining of SIRT1 (green) in major hypothalamic nuclei, including the PVN, SCN, Arc, VMH, DMH, and LH. Nuclei are counterstained by DAPI (gray). ***B***, Signal intensities of SIRT1 staining in hypothalami after 14 d DR compared to AL (*$p < 0.05$, **$p < 0.01$, $n = 4$ mice, 4–8 sections per hypothalamic nucleus). The signal intensity per area was digitally quantified after subtracting surrounding background. Results are shown as mean values ± SEM. ***C***, ***D***, cFOS staining in the DMH and LH after 14 d DR (***C***), and quantification of the number of cFOS-positive cells in hypothalamic nuclei (*$p < 0.05$, ***$p < 0.001$, $n = 4$ mice, 4–8 sections per hypothalamic nucleus). The numbers of cFOS-positive cells are shown as mean values ± SEM (***D***). ***E***, Transgene structure for the production of BRASTO mice (upper panel) and distribution of SIRT1 in major brain regions in both lines 1 and 10 of BRASTO mice (lower panels). ***F***, Immunofluorescent staining of SIRT1 (green) and HA (red) in hypothalami of BRASTO line 10. Nuclei are counterstained by DAPI (gray).

creases in SIRT1 protein expression in the brain (2.5- to 5.1- and 1.5- to 2.5-fold increases in lines 1 and 10, respectively) (Fig. 1*E*). There were ~2-fold increases in SIRT1 levels in the kidney in both lines and heart in line 1 (supplemental Fig. S4*A*, available at www.jneurosci.org as supplemental material). Interestingly, expression profiles of the overexpressed SIRT1 protein mimicked that of endogenous SIRT1 (Fig. 1*F*; supplemental Fig. S4*B*, available at www.jneurosci.org as supplemental material). Particularly in line 10, SIRT1 was overexpressed 2.7-fold in the DMH and 1.8-fold in the LH (supplemental Fig. S1*B*, right panel, available at www.jneurosci.org as supplemental material), a similar profile of increases in SIRT1 levels detected in the hypothalami of diet-

restricted wild-type mice (Fig. 1*B*). These BRASTO mice were born normally and did not show any gross abnormalities. We examined their fed and fasted plasma glucose and insulin levels, body weight, food intake, and glucose and insulin tolerance at the age of 5 months but did not detect any significant differences between BRASTO and control mice (supplemental Fig. S5, available at www.jneurosci.org as supplemental material).

BRASTO mice exhibit enhanced physical activity in response to diverse diet-restricting paradigms

During the course of our metabolic assessments, we noticed that BRASTO female mice were more active compared to control mice after 48 h fasting (supplemental Movies S1–4, available at www.jneurosci.org as supplemental material). When quantitated, BRASTO females in both lines 1 and 10 showed enhanced physical activity compared to control mice after 48 h fasting (WT vs Tg, line 1, $p = 0.008$; line 10, $p = 0.076$; percentage count, L1, $p = 0.002$; L10, $p = 0.060$) (Fig. 2*A*; supplemental Table S1, available at www.jneurosci.org as supplemental material). This phenotype was not obvious in BRASTO males, although there appears to be a similar trend, particularly in line 10 (supplemental Fig. S6*A*, available at www.jneurosci.org as supplemental material). Therefore, instead of an acute fasting condition, we evaluated the general locomotor activity in BRASTO and control males following a more chronic (14 d) DR condition. Interestingly, while diet-restricted BRASTO males showed a trend toward more total ambulations (whole-body movements) over a 24 h light/dark cycle, they exhibited significantly higher counts of rearing (vertical activity) compared to controls (light plus dark periods, $p = 0.049$; dark period alone, $p = 0.007$) (Fig. 2*B*). This increase in rearing activity was more obvious particularly during the dark period. Increases in rearing often signify heightened arousal levels and augmented environmental exploration and nonselective attention (Vallone et al., 2002). Therefore, these findings suggest that both BRASTO males and females have a greater propensity to increase their physical activity compared to control mice in response to diet-restricting conditions.

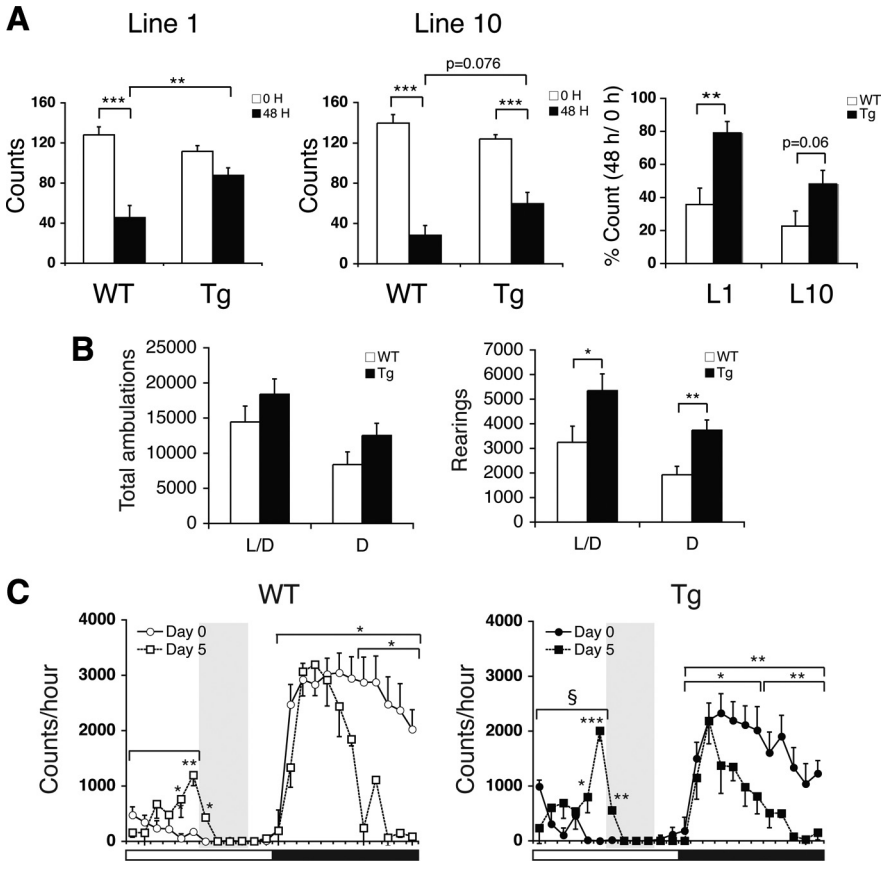

Figure 2. BRASTO mice exhibit enhanced physical activity in response to multiple diet-restricting paradigms. ***A***, Physical activity levels of BRASTO female mice after 48 h fasting in line 1 (left) and line 10 (middle). Activity counts (the numbers of quadrants crossed; left and middle) and percentage counts relative to the fed condition (right) are shown as mean values ± SEM (**$p < 0.01$, ***$p < 0.001$ by one-way ANOVA with Tukey–Kramer *post hoc* test, $n = 9$–12 mice). ***B***, Numbers of total ambulations (left) and rearings (right) of BRASTO (Tg) and control (WT) male mice in line 10 after 14 d DR are shown as mean values ± SEM (*$p < 0.05$, **$p < 0.01$, $n = 6$ mice). L/D, Light plus dark periods; D, dark period alone. ***C***, Wheel-running activity levels of BRASTO male mice in line 10 during a timed DR paradigm. Activity counts per hour through a 24 h light/dark cycle are shown. Shading represents feeding time (ZT6 to 10). Counts at each time point are shown as mean values ± SEM (day 0 vs day 5, *$p < 0.05$, **$p < 0.01$, ***$p < 0.001$ by paired Student's *t* or Wilcoxon matched-pairs signed-ranks tests; WT vs Tg, §$p < 0.05$ by a Wilcoxon matched-pairs signed-ranks test; $n = 5$–10 mice).

We also examined BRASTO and control mice in a different experimental paradigm in which they were fed daily from 1:00 P.M. (ZT6) to 5:00 P.M. (ZT10). In this timed DR paradigm, the food-anticipating activity (FAA) of mice significantly increases within several days of timed DR (Mistlberger, 1994; Stephan, 2002). Under this paradigm, BRASTO mice in both lines 1 and 10 exhibited enhanced FAA compared to control mice after 5 d of timed DR, although line 1 showed a much larger variability (supplemental Fig. S6*B*, available at www.jneurosci.org as supplemental material). Interestingly, BRASTO mice showed a greater increase in their FAA during ZT0–6 ($p = 0.03$) (Fig. 2*C*), particularly ZT5–6 right before feeding time, and a greater decrease in their night-time activity at ZT12–18 ($p = 0.047$) (Fig. 2*C*), supporting the idea that BRASTO mice might be able to reallocate their physical activity more efficiently than control mice, with the plausible purpose of seeking food. Together, these findings suggest that SIRT1 in the brain plays an important role in promoting physical activity in response to different diet-restricting conditions.

BRASTO mice show enhanced neural activation in the DMH and LH in response to diet-restricting conditions

We next examined which brain regions were more highly activated in BRASTO mice than in controls in response to different diet-restricting paradigms. In *ad libitum* conditions, there were only very small numbers of cFOS-positive cells in both wild-type and BRASTO hypothalami, except for the SCN that normally shows circadian rhythms of neural activation (Gooley et al., 2006), and no significant differences were observed between wild-type and BRASTO mice (supplemental Fig. S7*A*, available at www.jneurosci.org as supplemental material). After 48 h fasting, 90%, 46%, and 163% increases in the numbers of cFOS-positive cells were detected in the DMH, LH, and PVN of BRASTO mice,

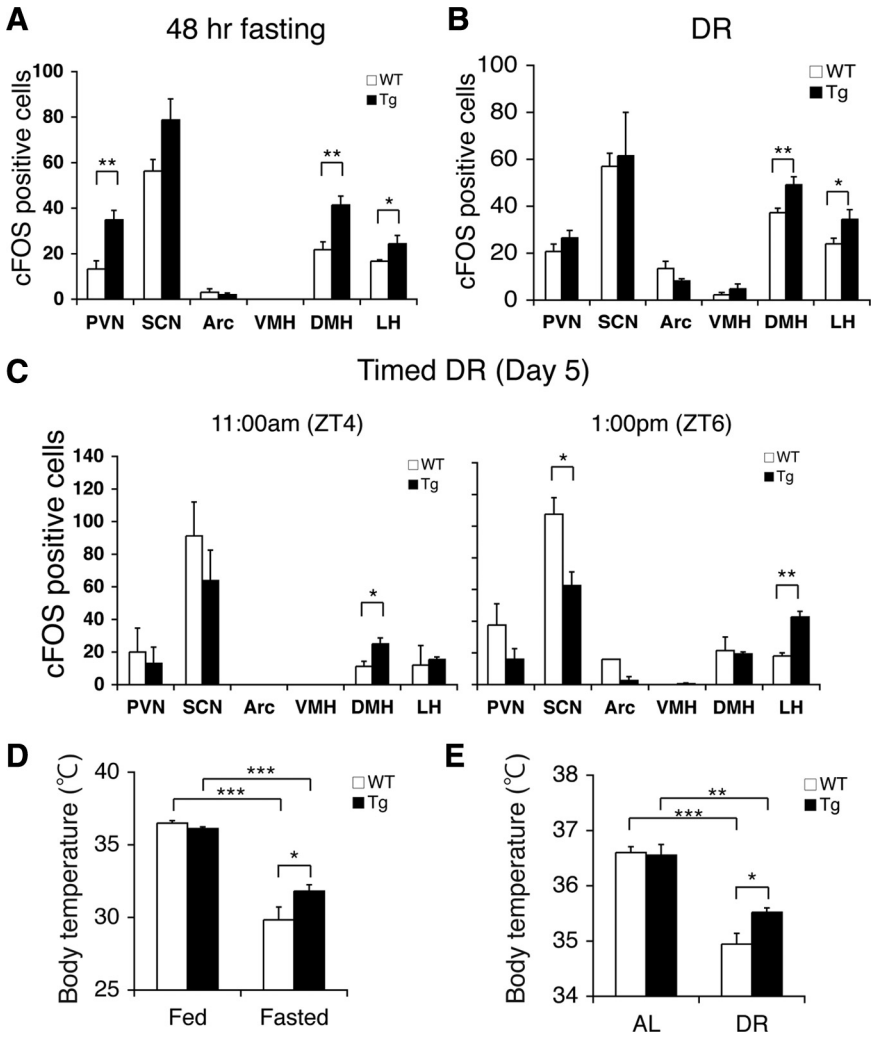

Figure 3. BRASTO mice show enhanced neural activation in the DMH and LH in response to multiple diet-restricting paradigms. ***A–C***, Quantification of cFOS-positive cells in major hypothalamic nuclei after 48 h fasting (***A***), 14 d DR (***B***), and 5 d of timed DR (***C***) in BRASTO mice in line 10 (*$p < 0.05$, **$p < 0.01$, $n = 4$ for 48 h fasting and DR, 4–8 sections per hypothalamic nucleus; $n = 2$ at each time point for timed DR, 2–5 sections per hypothalamic nucleus). The numbers of cFOS-positive cells are shown as mean values ± SEM. ***D***, ***E***, Rectal body temperature of BRASTO mice after 48 h fasting (***D***) and during 14 d DR (***E***). Levels of rectal body temperature are shown as mean values ± SEM (*$p < 0.05$, **$p < 0.01$, ***$p < 0.001$ by one-way ANOVA with Tukey–Kramer *post hoc* test, $n = 6$–7 for 48 h fasting, $n = 6$ for DR).

respectively, compared to those of control mice (DMH, $p = 0.0014$; LH, $p = 0.048$; PVN, $p = 0.002$) (Fig. 3*A*; supplemental Fig. S7*B*, available at www.jneurosci.org as supplemental material). The profile of the increases in cFOS-positive cells in hypothalamic nuclei of fasted BRASTO mice were very similar to those in diet-restricted wild-type mice (Fig. 1*D*), with the exception of the additional neural activation in the PVN. As the PVN is known to control the stress response through the stimulation of glucocorticoid secretion from adrenal glands, this additional PVN activation might correspond to a stress component imposed by sustained food anticipation under 48 h fasting. Indeed, a small but significant increase in plasma corticosterone levels was detected in fasted BRASTO females, compared to those in control fasted females (supplemental Fig. S8, available at www.jneurosci.org as supplemental material). After 14 d DR, the BRASTO DMH and LH exhibited 32% and 43% increases in the numbers of cFOS-positive cells, respectively, compared to those in control mice (DMH, $p = 0.008$; LH, $p = 0.049$) (Fig. 3*B*; supplemental Fig. S7*C*, available at www.jneurosci.org as supplemental material), whereas other hypothalamic nuclei did not show any significant differences between BRASTO and control mice, further supporting the importance of the DMH and LH in response to diet-restricting conditions. Because chow was always delivered between 4:00 P.M. and 5:00 P.M. in this DR regimen (see Materials and Methods), the observed activation of the DMH and LH does not appear to be related to the time of feeding. In the timed DR paradigm, 67% and 120% increases in the numbers of cFOS-positive cells were detected on day 5, first in the DMH and then in the LH of BRASTO mice, respectively, compared to those in control mice during the 2 h time course before feeding (DMH, $p = 0.034$; LH, $p = 0.002$) (Fig. 3*C*; supplemental Fig. S7*D*, available at www.jneurosci.org as supplemental material). The SCN is known to show circadian rhythms of neural activation peaking around ZT6 (Gooley et al., 2006). SIRT1 appears to suppress this oscillatory pattern, qualitatively consistent with the effect of SIRT1 on peripheral circadian rhythms (Nakahata et al., 2008; Ramsey et al., 2009). Thus, the most important point concerning these results is that the enhanced neural activation in the DMH and LH is tightly associated with increased physical activity in BRASTO mice under all three diet-restricting paradigms that we examined, namely, 48 h fasting, DR, and timed DR.

To further confirm that the observed enhancement of DMH and LH activation in BRASTO hypothalami is physiologically relevant, we examined rectal body temperature in BRASTO and control mice in response to 48 h fasting and DR. It has been demonstrated that neural activation in the DMH and LH plays an important role in the induction of thermogenesis in rodents (Cerri and Morrison, 2005; DiMicco and Zaretsky, 2007; Morrison et al., 2008). While both BRASTO and control mice showed significant decreases in rectal body temperature after 48 h fasting and 14 d DR, BRASTO mice were able to maintain higher levels of rectal body temperature compared to controls (WT vs Tg, fasted, $p = 0.032$; DR, $p = 0.023$) (Fig. 3*D*,*E*; supplemental Table S1, available at www.jneurosci.org as supplemental material), consistent with enhanced physical activity (Fig. 2*A*,*B*) and enhanced neural activation in the DMH and LH (Fig. 3*A*,*B*) in fasted and diet-restricted BRASTO mice. These results further support the importance of SIRT1 in the regulation of neural activation in the DMH and LH in response to different diet-restricting paradigms.

Sirt1-deficient mice exhibit defects in neurobehavioral adaptation to diet-restricting conditions

To examine whether SIRT1 is necessary for neurobehavioral adaptation to diet-restricting conditions, we decided to examine *Sirt1*-deficient ($Sirt1^{-/-}$) mice. Our $Sirt1^{-/-}$ mice were backcrossed to FVB. With this genetic background, $Sirt1^{-/-}$ mice

grow to adulthood with no significant early mortality (A.S., C.S.B., and S.I., unpublished observation), despite their previously reported small body size (Cheng et al., 2003; McBurney et al., 2003). We put these *Sirt1*$^{-/-}$ mice under a 14 d DR and examined the effects of this dietary change on their daily locomotor activity levels. Consistent with previously reported findings (Chen et al., 2005), diet-restricted *Sirt1*$^{-/-}$ mice failed to show significant increases in general ambulatory or rearing activity over a 24 h light/dark cycle, whereas diet-restricted *Sirt1*$^{+/+}$ mice significantly increased these indices of activity compared to levels observed during *ad libitum*-fed state (*Sirt1*$^{+/+}$ vs *Sirt1*$^{-/-}$, total ambulations in DR, $p = 0.03$; rearings in DR, $p = 0.037$) (Fig. 4*A*; supplemental Table S1, available at www.jneurosci.org as supplemental material) (Yu et al., 1985; Chen et al., 2005). Furthermore, *Sirt1*$^{-/-}$ mice only showed marginal increases in FAA compared to controls in the timed DR paradigm (ZT0–6, $p < 0.001$) (Fig. 4*B*).

We also compared levels of hypothalamic neural activation in *Sirt1*$^{-/-}$ and control mice under different diet-restricting conditions. In contrast to BRASTO mice, *Sirt1*$^{-/-}$ mice showed significantly lower numbers of cFOS-positive cells in both the DMH and LH compared to controls in response to 14 d DR (DMH, $p = 0.006$; LH, $p < 0.001$) (Fig. 4*C*, left panel). With this genetic background, we also detected a small but significant difference in the Arc between *Sirt1*$^{+/+}$ and *Sirt1*$^{-/-}$ mice. After 48 h fasting, the *Sirt1*$^{-/-}$ DMH also showed significantly lower numbers of cFOS-positive cells compared to the *Sirt1*$^{+/+}$ DMH, although the *Sirt1*$^{-/-}$ LH did not show a decrease in this genetic background and condition (DMH, $p = 0.011$; LH, $p = 0.611$) (Fig. 4*C*, middle panel). In the timed DR paradigm, a significant decrease in the number of cFOS-positive cells was again observed in the *Sirt1*$^{-/-}$ DMH at ZT4 ($p = 0.033$) (Fig. 4*C*, right panel). Consistent with lower levels of neural activation in the *Sirt1*$^{-/-}$ DMH and LH, *Sirt1*$^{-/-}$ mice were unable to maintain the range of rectal body temperature detected in *Sirt1*$^{+/+}$ mice in response to these diet-restricting conditions (*Sirt1*$^{+/+}$ vs *Sirt1*$^{-/-}$, DR, $p = 0.049$; fasted, $p < 0.001$) (Fig. 4*D*,*E*; supplemental Table S1, available at www.jneurosci.org as supplemental material). Together, these findings demonstrate that SIRT1 is necessary for the neurobehavioral adaptation to acute and chronic diet-restricting paradigms.

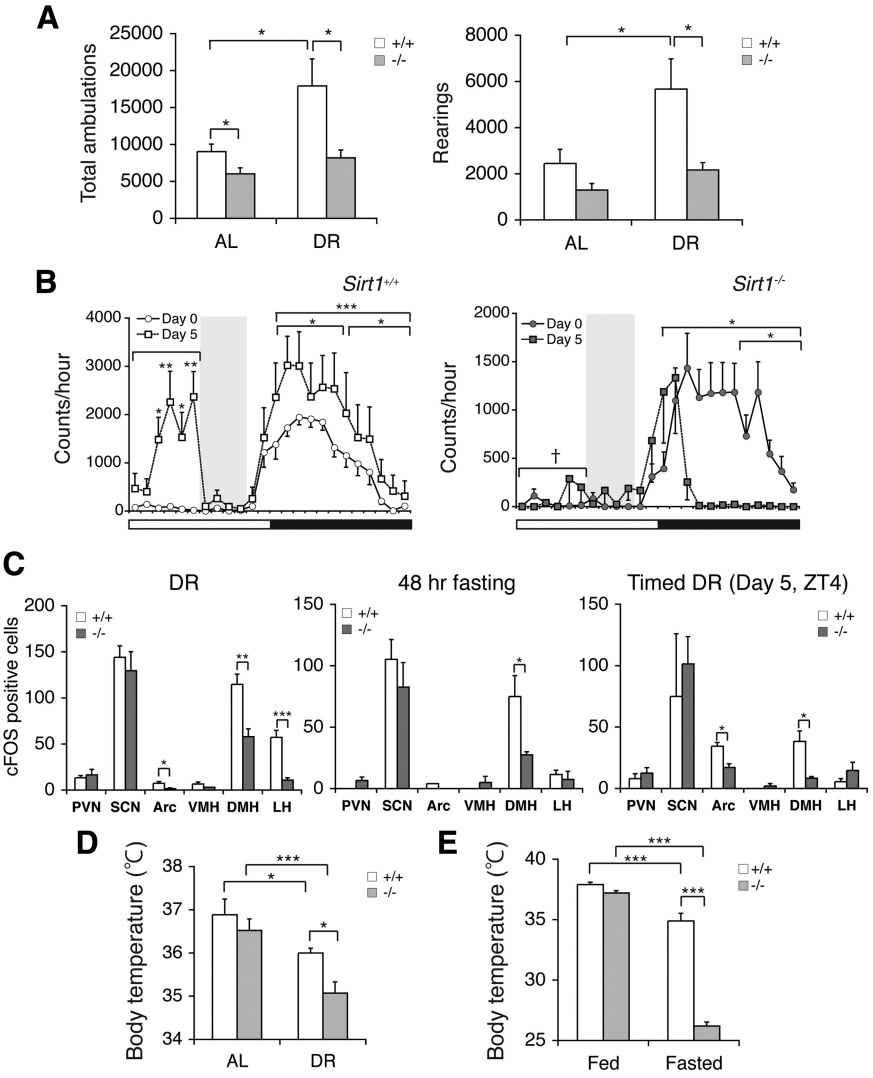

Figure 4. Sirt1-deficient mice have defects in neurobehavioral adaptation to diet-restricting conditions. ***A***, Numbers of total ambulations (left) and rearings (right) of *Sirt1*$^{+/+}$ and *Sirt1*$^{-/-}$ mice under AL and 14 d DR conditions are shown as mean values ± SEM (*$p < 0.05$ by one-way ANOVA with Tukey–Kramer *post hoc* test, $n = 5$ mice). ***B***, Wheel-running activity levels of *Sirt1*$^{-/-}$ and *Sirt1*$^{+/+}$ mice during a timed DR paradigm. Activity counts per hour of control mice (left) and *Sirt1*$^{-/-}$ mice (right) through a 24 h light/dark cycle are shown. Shading represents feeding time (ZT6 to 10). Counts at each time point are shown as mean values ± SEM (day 0 vs day 5, *$p < 0.05$, **$p < 0.01$, ***$p < 0.001$ by paired Student's *t* or Wilcoxon matched-pairs signed-ranks tests; *Sirt1*$^{+/+}$ vs *Sirt1*$^{-/-}$, $^{\dagger}p < 0.001$ by a Wilcoxon matched-pairs signed-ranks test, $n = 9$ and 4 for *Sirt1*$^{+/+}$ and *Sirt1*$^{-/-}$ mice, respectively). ***C***, Quantification of the number of cFOS-positive cells in hypothalamic nuclei after 14 d DR (left), 48 h fasting (middle), and 5 d of timed DR (right) in *Sirt1*$^{-/-}$ mice (*$p < 0.05$, **$p < 0.01$, ***$p < 0.001$, $n = 3$ mice for DR and fasting, 6–9 sections per hypothalamic nucleus; $n = 2$ mice for timed DR, 2–7 sections per hypothalamic nucleus). The numbers of cFOS-positive cells are shown as mean values ± SEM. ***D***, ***E***, Rectal body temperature of *Sirt1*$^{+/+}$ and *Sirt1*$^{-/-}$ mice during 14 d DR (***D***) and after 48 h fasting (***E***). Levels of rectal body temperature are shown as mean values ± SEM (*$p < 0.05$, ***$p < 0.001$ by one-way ANOVA with Tukey–Kramer *post hoc* test, $n = 5$–10 for 48 h fasting, $n = 5$ for DR).

SIRT1 upregulates genes that affect neural signaling and activity in the DMH and LH

To address the molecular mechanism by which SIRT1 promotes neural activation in the DMH and LH in response to diet-restricting conditions, we conducted microarray analyses to compare gene expression profiles between whole hypothalami from 48 h fasted BRASTO and control mice. Although none of the gene expression changes reached statistical significance in this particular experiment (data not shown), we noted that several genes previously reported to regulate neural signaling and activity might have important functional connections to the observed phenotypes in BRASTO mice, including the genes encoding orexin type 2 receptor (OX2R) (Sakurai et al., 1998), corticotropin releasing hormone receptor 1 (CRHR1) (Müller and Wurst, 2004), and Ca^{2+}-activated K^+ channel (BK) β2 subunit (KCNMB2) (Dai et al., 2009). We reexamined mRNA expression

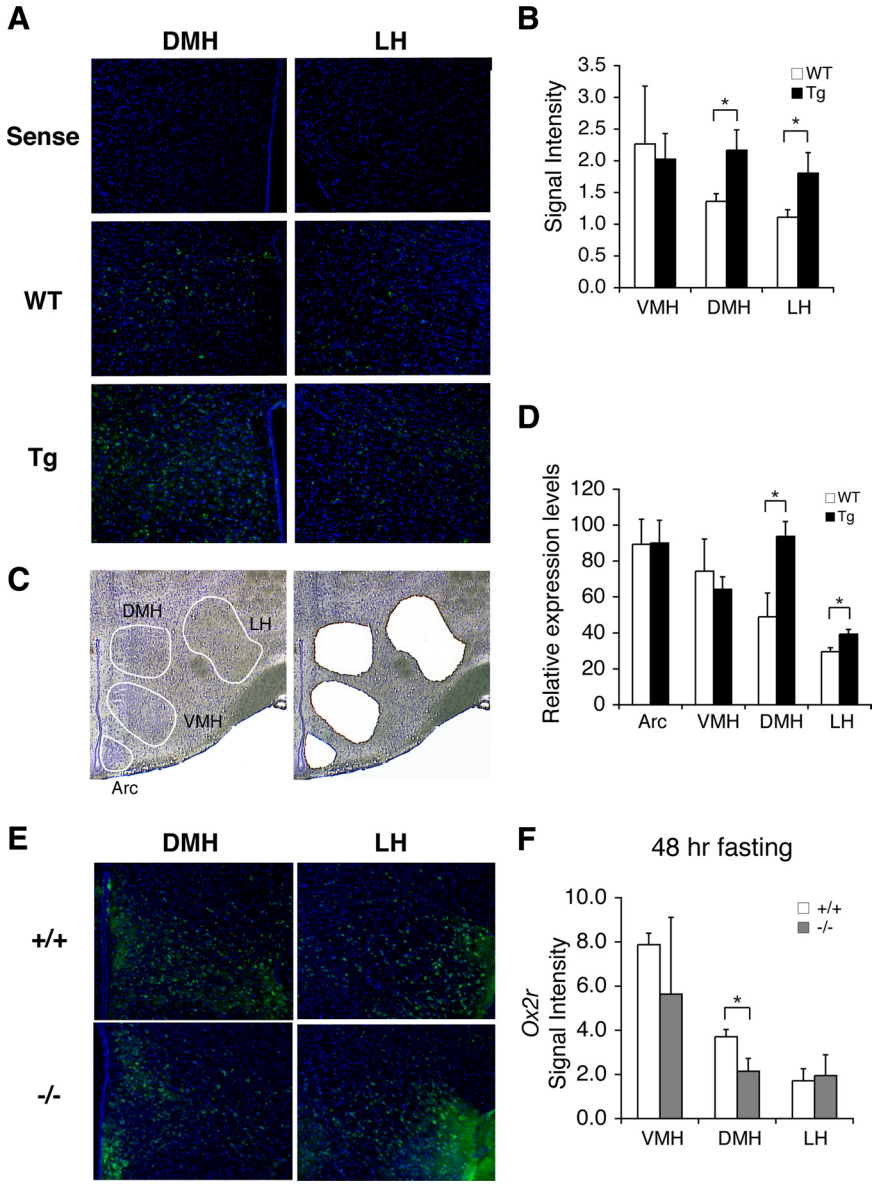

Figure 5. SIRT1 upregulates genes that affect neural signaling and activity in the DMH and LH. ***A***, The *in situ* hybridization of *Ox2r* (green) in the DMH and LH in BRASTO mice fasted for 48 h. Nuclei were counterstained by DAPI (blue). Upper panel, Sense probe hybridization on wild-type sections; middle and lower panels, antisense probe hybridization on wild-type (WT) and BRASTO (Tg) sections. ***B***, Quantification of signal levels of *Ox2r* mRNA in the VMH, DMH and LH. Results are shown as mean values ± SEM (*$p < 0.05$, $n = 3$–4 mice for each genotype, 3–8 sections per hypothalamic nucleus). ***C***, ***D***, Laser-microdissection of hypothalamic nuclei (***C***), and *Ox2r* expression levels in the Arc, VMH, DMH, and LH by real-time qRT-PCR (***D***). Results are shown as mean values ± SEM (*$p < 0.05$, $n = 4$ mice for each genotype). ***E***, ***F***, The *in situ* hybridization of *Ox2r* (green) in the DMH and LH in *Sirt1*$^{+/+}$ and *Sirt1*$^{-/-}$ mice fasted for 48 h (***E***), and signal levels of *Ox2r* mRNA in the VMH, DMH, and LH are shown as mean values ± SEM (***F***) (*$p < 0.05$, $n = 2$–3 mice for each genotype, 3–6 sections per hypothalamic nucleus).

levels of those genes in 48 h fasted BRASTO, *Sirt1*$^{-/-}$, and control mice by qRT-PCR. Interestingly, all three genes showed opposite directions of changes between BRASTO and *Sirt1*$^{-/-}$ mice (supplemental Fig. S9, available at www.jneurosci.org as supplemental material). In particular, *Ox2r* and *Kcnmb2* exhibited increases in BRASTO hypothalami and remarkable decreases in *Sirt1*$^{-/-}$ hypothalami, compared to respective controls. In contrast, the orexin type 1 receptor gene (*Ox1r*) (Sakurai et al., 1998) and the L-type voltage-gated Ca^{2+} channel subtype $Ca_v1.3$ gene, whose product is functionally coupled with BK channels (Berkefeld et al., 2006), did not show any changes in fasted BRASTO and *Sirt1*$^{-/-}$ hypothalami (supplemental Fig. S9, available at www.jneurosci.org as supplemental material). Given that only specific hypothalamic nuclei exhibited significant neural activation in BRASTO mice (Fig. 3*A–C*), we suspected that local changes in gene expression might be averaged out through the whole hypothalamus. To analyze such local changes in the expression of *Ox2r* and *Kcnmb2*, we conducted *in situ* hybridization through multiple independent brain sections from 48 h-fasted BRASTO and *Sirt1*$^{-/-}$ mice. More *Ox2r*-positive cells were clearly detected in the DMH and LH, but not in other hypothalamic nuclei, of BRASTO mice compared to those of wild-type controls (Fig. 5*A*). When assessing total signal levels in the VMH, DMH, and LH, *Ox2r* signal levels showed an ~80% increase selectively in the BRASTO DMH and LH relative to wild-type controls (DMH, $p = 0.02$; LH, $p = 0.028$) (Fig. 5*B*). qRT-PCR results with laser-microdissected samples of each hypothalamic nucleus also confirmed that *Ox2r* expression levels increased specifically in the BRASTO DMH and LH compared to wild-type controls (DMH, $p = 0.038$; LH, $p = 0.049$) (Fig. 5*C*,*D*), consistent with the observed enhancement of neural activation in the BRASTO DMH and LH under diet-restricting conditions (Fig. 3*A–C*). *Kcnmb2* signal levels increased in 48 h-fasted BRASTO hypothalami compared to control hypothalami, but this increase was not limited to the DMH and LH (supplemental Fig. S10, available at www.jneurosci.org as supplemental material). Conversely, fasted *Sirt1*$^{-/-}$ mice showed fewer *Ox2r*-positive cells and decreases in total *Ox2r* signal levels in the DMH, but not in the LH, compared to fasted *Sirt1*$^{+/+}$ mice (DMH, $p = 0.038$; LH, $p = 0.769$) (Fig. 5*E*,*F*), also consistent with significant decreases in neural activation in the DMH of fasted *Sirt1*$^{-/-}$ mice (Fig. 4*C*). Given that OX2R and orexin signaling have been reported to play an important role in the regulation of sleep, physical activity, and metabolism (Sakurai et al., 1998; Chemelli et al., 1999; Funato et al., 2009), these results suggest that the *Ox2r* gene might be a critical target of SIRT1 in the DMH and LH in response to diet-restricting conditions.

Diet restriction augments *Ox2r* expression in the DMH and LH through SIRT1

To test whether *Ox2r* expression is indeed induced by SIRT1 in response to DR, we examined *Ox2r* expression profiles in hypothalami of diet-restricted wild-type mice. Similar to the results in BRASTO hypothalami (Fig. 5*A*,*B*), DR increased the number of *Ox2r*-positive cells and total *Ox2r* signal levels significantly and specifically in the DMH and LH, but not in the VMH (DMH, $p = 0.002$; LH, $p = 0.028$; VMH, $p = 0.718$) (Fig. 6*A*,*B*). This DR-

induced enhancement of *Ox2r* expression was totally abrogated in the *Sirt1*$^{-/-}$ DMH and LH (DMH, $p = 0.013$; LH, $p = 0.015$; VMH, $p = 0.203$) (Fig. 6*C*,*D*), suggesting that SIRT1 is required for DR-induced enhancement of *Ox2r* expression in the DMH and LH. Furthermore, we found that SIRT1 was able to enhance the activity of the *Ox2r* promoter in a dose-dependent manner in cultured cells (1 μg, $p = 0.005$; 2 μg, $p < 0.001$) (Fig. 6*E*). To validate the relevance of this *in vitro* result, we also conducted chromatin-immunoprecipitation (ChIP) assays with isolated mouse hypothalami to examine whether SIRT1 resides in the *Ox2r* promoter region *in vivo*. ChIP analyses revealed that SIRT1 resided specifically in the *Ox2r* proximal promoter region spanning from −110 bp to −457 bp (Fig. 6*F*). Thus, these findings suggest that increased SIRT1 activity in BRASTO and diet-restricted hypothalami enhances *Ox2r* expression and promotes neural activation specifically in the DMH and LH, which tightly correlates with enhanced physical activity in response to diet-restricting conditions.

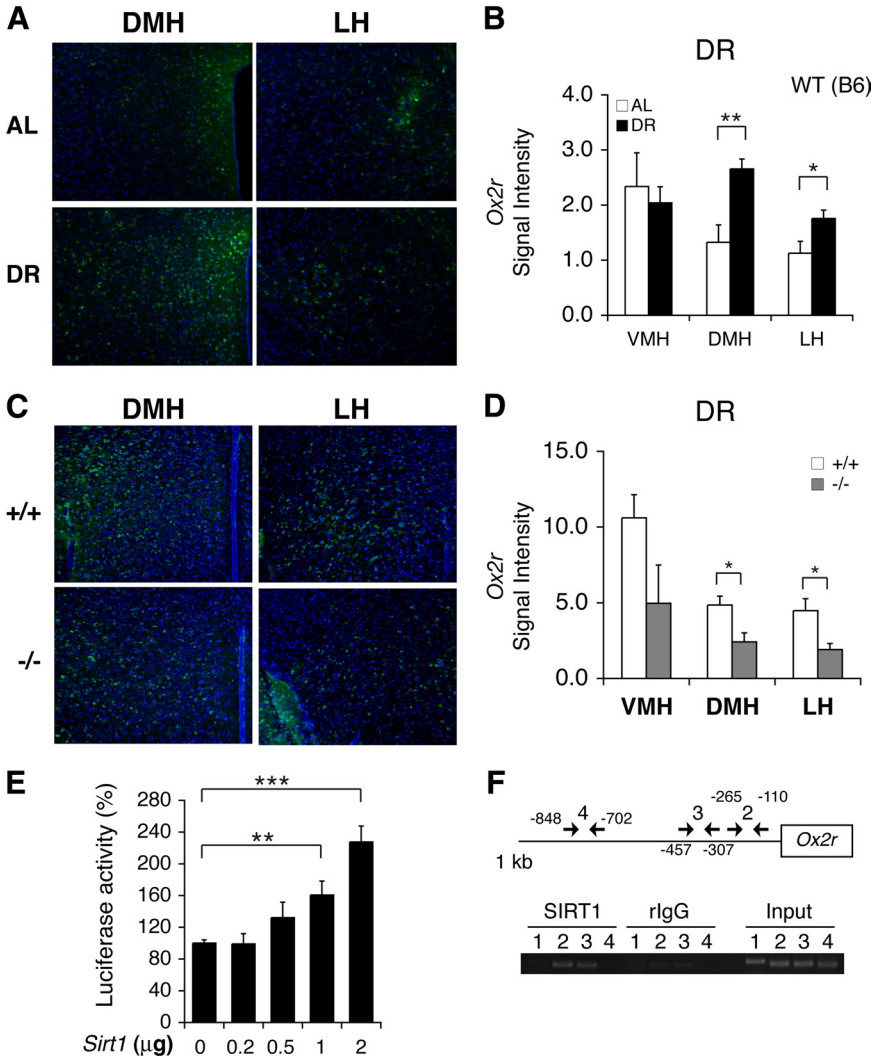

Figure 6. Diet restriction augments *Ox2r* expression in the DMH and LH via SIRT1. ***A–D***, *In situ* hybridization of *Ox2r* in the DMH and LH in wild-type C57BL/6 male mice (***A***, ***B***) and *Sirt1*$^{-/-}$ FVB male mice (***C***, ***D***) under 14 d DR. *Ox2r* signal levels were quantified in each hypothalamic nucleus under AL and 14 d DR (***B***) and between diet-restricted *Sirt1*$^{+/+}$ and *Sirt1*$^{-/-}$ mice (***D***). The signal intensity per area was digitally quantified after subtracting surrounding background. Results are shown as mean values ± SEM (*$p < 0.05$, **$p < 0.01$, $n = 3–4$ each for AL and DR mice (4–10 sections and per hypothalamic nucleus) and for *Sirt1*$^{+/+}$ and *Sirt1*$^{-/-}$ mice (2–8 sections per hypothalamic nucleus)). ***E***, Luciferase activities were measured by transfecting HEK293 cells with a luciferase reporter driven by a ~1 kb *Ox2r* promoter and a *Sirt1* minigene or a control vector carrying only the *Sirt1* promoter. Luciferase activities were compared with increasing amounts of the *Sirt1* minigene. The luciferase activities in cells transfected with the promoter-only control vector are normalized to 100%. Results are shown as mean values ± SEM (**$p < 0.01$, ***$p < 0.001$ by one-way ANOVA with Tukey–Kramer *post hoc* test, $n = 4$). ***F***, Chromatin immunoprecipitation for SIRT1 in the hypothalamus. Fixed chromatin was sonicated and subjected to immunoprecipitation with an anti-SIRT1 polyclonal antibody. Extracted DNA was amplified with each primer set. Primer set 1 was designed for an unrelated genomic region. Locations of primer sets 2–4 are shown in the upper panel. Rabbit IgG (rIgG) was used as a negative control.

The gut hormone ghrelin induces enhanced neural activation in BRASTO hypothalami

Because DR apparently imposes a signal that stimulates DMH and LH neurons in both wild-type and BRASTO mice, we suspected that some hormones produced in peripheral tissues in response to DR might generate such a stimulatory signal in the hypothalamus. We were particularly interested in ghrelin, an orexigenic hormone secreted from stomach, because ghrelin has been reported to stimulate orexin neurons in LH (Horvath et al., 2001) and in culture (Yamanaka et al., 2003). It has also been shown that peripheral injection of ghrelin increases the number of cFOS-positive cells in the DMH in rats (Kobelt et al., 2008). Therefore, we hypothesized that ghrelin contributes to the peripheral signal responsible for stimulating DMH and LH neurons in response to DR in wild-type and BRASTO mice. We first examined serum ghrelin levels in AL and diet-restricted mice. Ghrelin levels significantly increased in mice under DR, compared to those in AL mice ($p = 0.006$) (Fig. 7*A*, left). Ghrelin levels also increased similarly in both 48 h fasted control and BRASTO mice (WT, $p < 0.001$; Tg, $p < 0.001$) (Fig. 7*A*, right; supplemental Table S1, available at www.jneurosci.org as supplemental material). We next compared neural activation in control and BRASTO hypothalami to peripheral ghrelin injection. After 4 d of habituation to handling and mock injection to avoid stress-induced neural activation, we injected PBS or ghrelin intraperitoneally into both control and BRASTO mice. Whereas control PBS injection showed minimal cFOS induction with no baseline differences between wild-type and BRASTO mice, ghrelin induced cFOS-positive cells in the Arc, DMH, and LH over 2 h after injection, and the BRASTO DMH and LH showed significantly higher numbers of cFOS-positive cells than control DMH and LH after ghrelin injection (WT vs Tg, DMH, $p = 0.017$; LH, $p = 0.019$) (Fig. 7*B*). Consistent with this DMH- and LH-specific enhancement of neural activation in BRASTO mice, they were also able to maintain higher levels of rectal body temperature compared to controls after ghrelin injection (WT vs Tg, $p = 0.048$) (Fig. 7*C*; supplemental Table S1, available at www.jneurosci.org as supplemental material), which mimics the changes in rectal body temperature observed in diet-restricted wild-type and BRASTO mice (Fig. 3*E*). Interestingly, the majority of cFOS-positive cells were

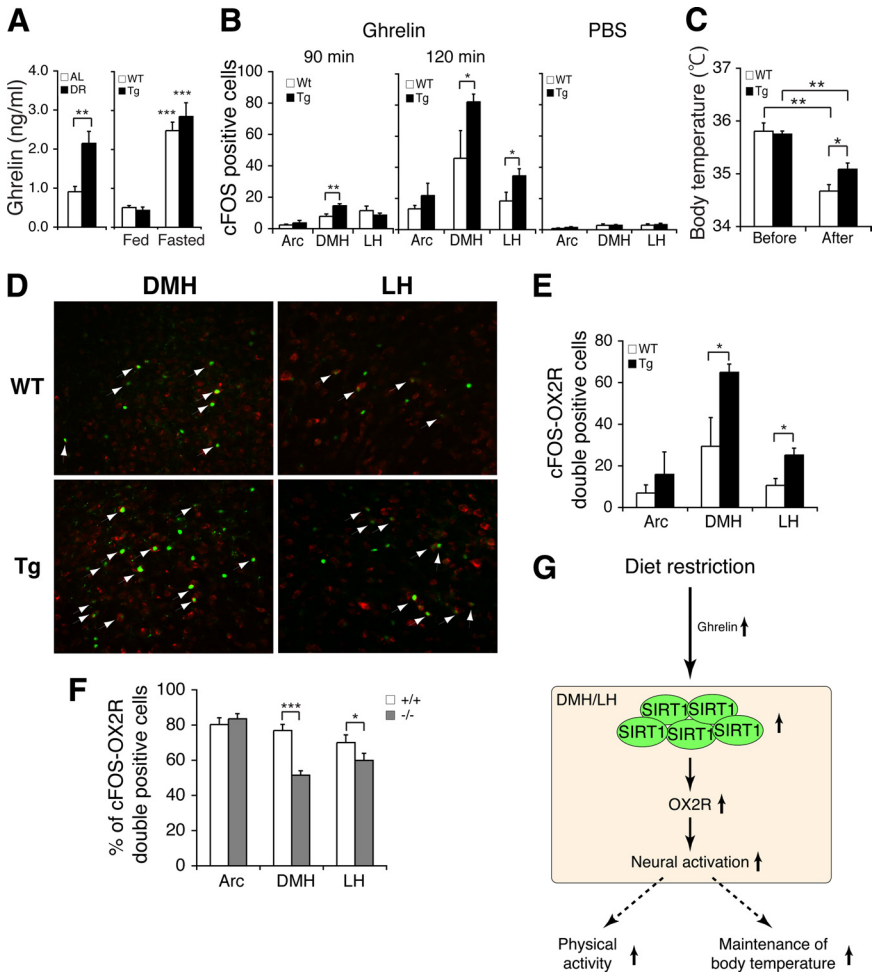

Figure 7. Ghrelin stimulates OX2R-positive neurons in the BRASTO DMH and LH, but not in *Sirt1*-deficient mice. ***A***, Serum levels of ghrelin in AL and DR wild-type mice (left) and in fed and fasted BRASTO (Tg) and control (WT) mice (right). Ghrelin levels are shown as mean values ± SEM (**$p < 0.01$, ***$p < 0.001$ by one-way ANOVA with Tukey–Kramer *post hoc* test, $n = 5$ for each condition). ***B***, The number of cFOS-positive cells in the Arc, DMH, and LH of wild-type (WT) and BRASTO (Tg) mice at 90 min (left) and 120 min (right) after ghrelin injection (30 nmol/kg of body weight) and after PBS injection (right). cFOS-positive cells are shown as mean values ± SEM (*$p < 0.05$, **$p < 0.01$ by one-way ANOVA with Tukey–Kramer *post hoc* test for each hypothalamic nucleus, ghrelin injection, 90 min, $n = 2$–3 mice for each genotype, 7–12 sections per hypothalamic nucleus; 120 min, $n = 3$ for each genotype, 3–7 sections per hypothalamic nucleus, PBS injection, $n = 2$ for each genotype, 6–7 sections per hypothalamic nucleus). ***C***, Rectal body temperature of BRASTO mice 120 min after ghrelin injection. Levels of rectal body temperature are shown as mean values ± SEM (*$p < 0.05$, **$p < 0.01$ by one-way ANOVA with Tukey–Kramer *post hoc* test, $n = 6$–7). ***D***, Double immunofluorescent staining of cFOS and OX2R in the DMH and LH of wild-type (WT) and BRASTO (Tg) mice at 120 min after ghrelin injection. Arrows indicate cFOS/OX2R-double-positive cells. ***E***, Quantification of the number of cFOS/OX2R-double-positive cells in the Arc, DMH and LH of wild-type (WT) and BRASTO (Tg) mice at 120 min after ghrelin injection. cFOS/OX2R-double-positive cells are shown as mean values ± SEM (*$p < 0.05$, $n = 3$ mice for each genotype, 3–7 sections per hypothalamic nucleus). ***F***, Percentage of cFOS/OX2R-double-positive cells compared to a total number of cFOS-positive cells in the Arc, DMH, and LH of *Sirt1*$^{+/+}$ and *Sirt1*$^{-/-}$ mice at 120 min after ghrelin injection. Percentages of cFOS/OX2R-double-positive cells are shown as mean values ± SEM (*$p < 0.05$, ***$p < 0.001$, $n = 3$ mice for each genotype, 6–12 sections per hypothalamic nucleus). ***G***, A model for the SIRT1-mediated neurobehavioral adaptation in the hypothalamus in response to DR. See Discussion for details.

also OX2R-positive (82 and 72% in the Arc, 77 and 79% in the DMH, and 57 and 72% in the LH in control and BRASTO mice, respectively, at 120 min after ghrelin injection) (Fig. 7*D*), and the numbers of cFOS/OX2R-double-positive cells were significantly higher in the BRASTO DMH and LH compared to controls at 120 min after ghrelin injection (DMH, $p = 0.015$; LH, $p = 0.012$) (Fig. 7*E*). We also examined the response of *Sirt1*$^{+/+}$ and *Sirt1*$^{-/-}$ mice to peripheral ghrelin injection. Among all activated neurons, the percentages of cFOS/OX2R-double-positive cells were significantly lower in the *Sirt1*$^{-/-}$ DMH and LH (DMH, $p < 0.001$; LH, $p = 0.042$) (Fig. 7*F*), suggesting that the response to ghrelin through OX2R is significantly reduced in the *Sirt1*$^{-/-}$ LH and DMH. Together, our findings indicate that peripheral ghrelin, whose levels are significantly increased by diet-restricting conditions, triggers the stimulatory signal in the DMH and LH where SIRT1 enhances the responsiveness of neurons through the augmentation of *Ox2r* expression.

Discussion

SIRT1 functions as a key mediator for the central adaptation to diet restriction

In this study, we provide several lines of evidence demonstrating the physiological significance of SIRT1 in the regulation of neurobehavioral adaptation to DR: (1) SIRT1 protein levels and neural activation are induced specifically in the DMH and LH by DR, (2) increased SIRT1 dosage in the brain significantly enhances neural activation in the DMH and LH, maintains a higher range of body temperature, and promotes physical activity in BRASTO mice in response to multiple diet-restricting paradigms, (3) these responses induced by diet-restricting conditions are abrogated by SIRT1 deficiency, (4) SIRT1 is required for the DR-induced enhancement of *Ox2r* expression in the DMH and LH and is also able to enhance the promoter activity of the *Ox2r* gene, and (5) ghrelin, a gut hormone whose plasma levels are significantly increased by both 48 h fasting and DR, stimulates OX2R-positive neurons in the DMH and LH and maintains higher body temperature in BRASTO mice, while *Sirt1*$^{-/-}$ mice show significantly reduced neural activation through OX2R in the DMH and LH. These findings suggest that SIRT1 controls a central adaptive mechanism by which animals maintain their physical activity and body temperature in response to relatively chronic energy limitation. Given that BRASTO mice show an enhancement of these neurobehavioral responses to DR, whereas *Sirt1*$^{-/-}$ mice exhibit defects in these responses, persistent low energy intake such as DR likely triggers this adaptive mechanism by augmenting SIRT1 activity and thereby *Ox2r* expression, at least in part, in the DMH and LH and enhancing the sensitivity of OX2R-positive neurons to signals imposed possibly by peripheral ghrelin.

A novel central connection between SIRT1 and OX2R-mediated orexin signaling

Our finding that SIRT1 enhances *Ox2r* expression specifically in the DMH and LH in response to DR illustrates a novel central connection between two key players in the regulation of metabolism and behavior. Orexin-OX1/2R signaling has been demonstrated to play a critical role in the central regulation of arousal,

motivational components of physical activity, and metabolism (Sakurai et al., 1998; Chemelli et al., 1999; Funato et al., 2009). In particular, hypothalamic orexin signaling plays an essential role in the fasting-induced enhancement of wakefulness and locomotor activity (Yamanaka et al., 2003). It has also been shown that orexin neuron-ablated mice have a severe defect in the food-anticipatory enhancement of wakefulness and locomotor activity under timed DR (Mieda et al., 2004). It has recently been demonstrated that orexin-OX2R signaling regulates metabolic rate, food intake, and leptin and insulin sensitivity and thereby conveys resistance to high-fat diet-induced metabolic complications (Funato et al., 2009). Thus, hypothalamic orexin signaling functions as a critical mediator of central adaptive responses to alterations in energy intake.

Similarly, it has been well established that SIRT1 mediates a variety of critical metabolic effects in response to nutritional cues, particularly to low nutritional input, in major metabolic tissues, such as liver, adipose tissue, and skeletal muscle (Sinclair, 2005; Imai and Guarente, 2007; Schwer and Verdin, 2008; Imai and Guarente, 2010). Most recently, it has been reported that pharmacological inhibition or Arc-specific knockdown of hypothalamic SIRT1 suppresses food intake and body weight gain, likely through the central melanocortin signaling, in rats (Cakir et al., 2009). SIRT1 is expressed in pro-opiomelanocortin (POMC) neurons (Ramadori et al., 2008) and appears to regulate *Pomc* expression through deacetylation of FOXO1 (Cakir et al., 2009). These studies reveal hypothalamic SIRT1 function in response to acute nutritional deprivation. Our present study further extends this interesting aspect of SIRT1 function in the hypothalamus and reveals a new metabolic role of SIRT1 in different hypothalamic nuclei, namely the DMH and LH, in response to more chronic nutritional alterations. SIRT1 appears to control the sensitivity of a particular subset of neurons in the DMH and LH through the regulation of *Ox2r* expression and makes them more responsive to increased ghrelin signal under DR (Fig. 7*G*). Because ghrelin directly stimulates orexin neurons (Horvath et al., 2001; Yamanaka et al., 2003), it is highly likely that those OX2R-positive DMH and LH neurons are stimulated by the orexin neurons that are activated by ghrelin (Fig. 7*G*). Although further investigation will be necessary to clarify the entire signaling cascade, the augmentation of OX2R-mediated neural activation in response to DR appears to be accomplished by the localized increase in SIRT1 protein levels in the DMH and LH. Nonetheless, because BRASTO mice do not show significant phenotypes in AL conditions, hypothalamic SIRT1 activity might also be augmented by increased systemic NAD biosynthesis or other mechanisms activated by low nutritional input, as reported in other cases (Cakir et al., 2009; Imai, 2009b). Detailed analyses are currently underway to elucidate the molecular mechanism by which SIRT1 augments *Ox2r* expression specifically in the DMH and LH in response to low nutritional input.

The SIRT1-mediated systemic regulatory network for adaptive responses to diet restriction

It should be noted that persistent neural activation is observed in the DMH and LH under DR, although other hypothalamic nuclei, such as the Arc and VMH, might be involved in regulatory processes that trigger metabolic changes at an early stage during DR. Our findings suggest that SIRT1 in the OX2R-positive DMH and LH neurons might play a critical role in coordinating metabolic responses to chronic diet-restricting conditions at a systemic level. Although their precise nature is currently unclear, the activation of these OX2R-positive DMH and LH neurons leads to the stimulation of thermogenesis and the elevation of physical activity in response to relatively chronic diet-restricting conditions. Increasing SIRT1 dosage further promotes these responses, whereas SIRT1 deficiency abrogates them. Given that it has been shown that DMH and LH neurons regulate thermogenesis in brown adipose tissue through the control of sympathetic nerve activity (Cerri and Morrison, 2005; DiMicco and Zaretsky, 2007; Morrison et al., 2008), it is tempting to speculate that SIRT1 activity in these neurons might affect such systemic responses through the regulation of sympathetic nerve activity. However, in light of the complexity of hypothalamic circuits, the fact that some hypothalamic nuclei appear to be more homogeneous than others in their responses does not necessarily allow us to conclude that those particular nuclei are central in such systemic responses. Definitive tests await the generation of necessary genetic tools, such as DMH- or LH-specific Cre-driver mice. Nonetheless, it will also be of great importance to examine where these OX2R-positive DMH and LH neurons send their projections and which neurons control activities of those DMH and LH neurons.

It is conceivable that those specific hypothalamic neurons, as well as other hypothalamic neurons such as AgRP and POMC neurons, might also be important for age-associated alterations in neurobehavioral adaptive responses to nutritional inputs and possibly for longevity as well in mammals, given that it has been demonstrated that a very specific subset of sensory neurons, namely SKN-1-positive neurons, mediates DR-induced longevity through an endocrine mechanism in *C. elegans* (Bishop and Guarente, 2007b). Such a hierarchical regulatory network might play a universal role in the regulation of aging and longevity in animals, and SIRT1 might be an integral component in the DMH and LH to modulate systemic signals in response to changes in energy intake in mammals. Indeed, peripheral administration of ghrelin, an orexigenic hormone produced in the stomach, triggers the activation of the DMH and LH neurons and induces changes in body temperature, mimicking the effect of DR. Increased SIRT1 dosage enhances this neural response to ghrelin and allows animals to maintain a higher range of body temperature. Therefore, SIRT1 might function as a critical modulator in this hierarchical regulatory network for the regulation of central adaptive responses. Alteration in SIRT1 activity in these neurons might cause significant changes in the system dynamics of this adaptive mechanism. In this regard, it is intriguing that systemic NAD biosynthesis appears to decline over age, resulting in reductions in SIRT1 activity and glucose-stimulated insulin secretion in pancreatic β cells in aged mice (Ramsey et al., 2008; Imai, 2009b). Such an age-associated decrease in systemic NAD biosynthesis might contribute to the alteration of certain neurobehavioral adaptations, such as reduced motivation for activity and sleep disorders, both of which are common in the elderly (Kmiec, 2006).

In conclusion, our present study demonstrates the physiological significance of SIRT1 as a key central mediator for the neurobehavioral adaptation to DR. These findings provide critical insights into the molecular mechanism by which mammals control their neurobehavioral adaptive responses to search for food and to survive through diet-restricted, life-threatening environments.

References

Anderson RM, Bitterman KJ, Wood JG, Medvedik O, Sinclair DA (2003) Nicotinamide and PNC1 govern lifespan extension by calorie restriction in *Saccharomyces cerevisiae*. Nature 423:181–185.

Aton SJ, Block GD, Tei H, Yamazaki S, Herzog ED (2004) Plasticity of cir-

cadian behavior and the suprachiasmatic nucleus following exposure to non-24-hour light cycles. J Biol Rhythms 19:198–207.
Berkefeld H, Sailer CA, Bildl W, Rohde V, Thumfart JO, Eble S, Klugbauer N, Reisinger E, Bischofberger J, Oliver D, Knaus HG, Schulte U, Fakler B (2006) BKCa-Cav channel complexes mediate rapid and localized Ca2+-activated K+ signaling. Science 314:615–620.
Bishop NA, Guarente L (2007a) Genetic links between diet and lifespan: shared mechanisms from yeast to humans. Nat Rev Genet 8:835–844.
Bishop NA, Guarente L (2007b) Two neurons mediate diet-restriction-induced longevity in *C. elegans*. Nature 447:545–549.
Bronson RT, Lipman RD (1991) Reduction in rate of occurrence of age related lesions in dietary restricted laboratory mice. Growth Dev Aging 55:169–184.
Cakir I, Perello M, Lansari O, Messier NJ, Vaslet CA, Nillni EA (2009) Hypothalamic Sirt1 regulates food intake in a rodent model system. PLoS ONE 4:e8322.
Cerri M, Morrison SF (2005) Activation of lateral hypothalamic neurons stimulates brown adipose tissue thermogenesis. Neuroscience 135:627–638.
Chapman T, Partridge L (1996) Female fitness in *Drosophila melanogaster*: an interaction between the effect of nutrition and of encounter rate with males. Proc Biol Sci 263:755–759.
Chemelli RM, Willie JT, Sinton CM, Elmquist JK, Scammell T, Lee C, Richardson JA, Williams SC, Xiong Y, Kisanuki Y, Fitch TE, Nakazato M, Hammer RE, Saper CB, Yanagisawa M (1999) Narcolepsy in orexin knockout mice: molecular genetics of sleep regulation. Cell 98:437–451.
Chen D, Steele AD, Lindquist S, Guarente L (2005) Increase in activity during calorie restriction requires Sirt1. Science 310:1641.
Chen D, Steele AD, Hutter G, Bruno J, Govindarajan A, Easlon E, Lin SJ, Aguzzi A, Lindquist S, Guarente L (2008) The role of calorie restriction and SIRT1 in prion-mediated neurodegeneration. Exp Gerontol 43:1086–1093.
Cheng HL, Mostoslavsky R, Saito S, Manis JP, Gu Y, Patel P, Bronson R, Appella E, Alt FW, Chua KF (2003) Developmental defects and p53 hyperacetylation in Sir2 homolog (SIRT1)-deficient mice. Proc Natl Acad Sci U S A 100:10794–10799.
Colman RJ, Anderson RM, Johnson SC, Kastman EK, Kosmatka KJ, Beasley TM, Allison DB, Cruzen C, Simmons HA, Kemnitz JW, Weindruch R (2009) Caloric restriction delays disease onset and mortality in rhesus monkeys. Science 325:201–204.
Dai S, Hall DD, Hell JW (2009) Supramolecular assemblies and localized regulation of voltage-gated ion channels. Physiol Rev 89:411–452.
DiMicco JA, Zaretsky DV (2007) The dorsomedial hypothalamus: a new player in thermoregulation. Am J Physiol Regul Integr Comp Physiol 292:R47–R63.
Dragunow M, Faull R (1989) The use of c-fos as a metabolic marker in neuronal pathway tracing. J Neurosci Methods 29:261–265.
Elmquist JK (2001) Hypothalamic pathways underlying the endocrine, autonomic, and behavioral effects of leptin. Physiol Behav 74:703–708.
Fontana L, Meyer TE, Klein S, Holloszy JO (2004) Long-term calorie restriction is highly effective in reducing the risk for atherosclerosis in humans. Proc Natl Acad Sci U S A 101:6659–6663.
Funato H, Tsai AL, Willie JT, Kisanuki Y, Williams SC, Sakurai T, Yanagisawa M (2009) Enhanced orexin receptor-2 signaling prevents diet-induced obesity and improves leptin sensitivity. Cell Metab 9:64–76.
Gooley JJ, Schomer A, Saper CB (2006) The dorsomedial hypothalamic nucleus is critical for the expression of food-entrainable circadian rhythms. Nat Neurosci 9:398–407.
Green CB, Takahashi JS, Bass J (2008) The meter of metabolism. Cell 134:728–742.
Horvath TL, Diano S, Sotonyi P, Heiman M, Tschöp M (2001) Minireview: ghrelin and the regulation of energy balance—a hypothalamic perspective. Endocrinology 142:4163–4169.
Imai S (2009a) SIRT1 and caloric restriction: an insight into possible trade-offs between robustness and frailty. Curr Opin Clin Nutr Metab Care 12:350–356.
Imai S (2009b) The NAD world: a new systemic regulatory network for metabolism and aging—Sirt1, systemic NAD biosynthesis, and their importance. Cell Biochem Biophys 53:65–74.
Imai S, Guarente L (2007) Sirtuins: a universal link between NAD, metabolism, and aging. In: The molecular biology of aging (Guarente L, Partridge L, Wallace D, eds), pp 39–72. New York: Cold Spring Harbor Laboratory.
Imai S, Guarente L (2010) Ten years of NAD-dependent SIR2 family deacetylases: implications for metabolic diseases. Trends Pharmacol Sci 31:212–220.
Imai S, Armstrong CM, Kaeberlein M, Guarente L (2000) Transcriptional silencing and longevity protein Sir2 is an NAD-dependent histone deacetylase. Nature 403:795–800.
Ingram DK, Weindruch R, Spangler EL, Freeman JR, Walford RL (1987) Dietary restriction benefits learning and motor performance of aged mice. J Gerontol 42:78–81.
Kaeberlein M, McVey M, Guarente L (1999) The *SIR2/3/4* complex and *SIR2* alone promote longevity in *Saccharomyces cerevisiae* by two different mechanisms. Genes Dev 13:2570–2580.
Kmiec Z (2006) Central regulation of food intake in ageing. J Physiol Pharmacol 57 [Suppl 6]:7–16.
Kobelt P, Wisser AS, Stengel A, Goebel M, Inhoff T, Noetzel S, Veh RW, Bannert N, van der Voort I, Wiedenmann B, Klapp BF, Taché Y, Mönnikes H (2008) Peripheral injection of ghrelin induces Fos expression in the dorsomedial hypothalamic nucleus in rats. Brain Res 1204:77–86.
Lakowski B, Hekimi S (1998) The genetics of caloric restriction in *Caenorhabditis elegans*. Proc Natl Acad Sci U S A 95:13091–13096.
Lin S-J, Defossez P-A, Guarente L (2000) Life span extension by calorie restriction in *S. cerevisiae* requires NAD and *SIR2*. Science 289:2126–2128.
Masoro EJ (2005) Overview of caloric restriction and ageing. Mech Ageing Dev 126:913–922.
McBurney MW, Yang X, Jardine K, Hixon M, Boekelheide K, Webb JR, Lansdorp PM, Lemieux M (2003) The mammalian SIR2alpha protein has a role in embryogenesis and gametogenesis. Mol Cell Biol 23:38–54.
McCay CM, Crowell MF, Maynard LA (1935) The effect of retarded growth upon the length of life span and upon the ultimate body size. J Nutr 10:63–79.
Mieda M, Williams SC, Sinton CM, Richardson JA, Sakurai T, Yanagisawa M (2004) Orexin neurons function in an efferent pathway of a food-entrainable circadian oscillator in eliciting food-anticipatory activity and wakefulness. J Neurosci 24:10493–10501.
Mistlberger RE (1994) Circadian food-anticipatory activity: formal models and physiological mechanisms. Neurosci Biobehav Rev 18:171–195.
Morrison SF, Nakamura K, Madden CJ (2008) Central control of thermogenesis in mammals. Exp Physiol 93:773–797.
Moynihan KA, Grimm AA, Plueger MM, Bernal-Mizrachi E, Ford E, Cras-Méneur C, Permutt MA, Imai S (2005) Increased dosage of mammalian Sir2 in pancreatic β cells enhances glucose-stimulated insulin secretion in mice. Cell Metab 2:105–117.
Müller MB, Wurst W (2004) Getting closer to affective disorders: the role of CRH receptor systems. Trends Mol Med 10:409–415.
Nakahata Y, Kaluzova M, Grimaldi B, Sahar S, Hirayama J, Chen D, Guarente LP, Sassone-Corsi P (2008) The NAD+-dependent deacetylase SIRT1 modulates CLOCK-mediated chromatin remodeling and circadian control. Cell 134:329–340.
Ramadori G, Lee CE, Bookout AL, Lee S, Williams KW, Anderson J, Elmquist JK, Coppari R (2008) Brain SIRT1: anatomical distribution and regulation by energy availability. J Neurosci 28:9989–9996.
Ramsey KM, Mills KF, Satoh A, Imai S (2008) Age-associated loss of Sirt1-mediated enhancement of glucose-stimulated insulin secretion in β cell-specific Sirt1-overexpressing (BESTO) mice. Aging Cell 7:78–88.
Ramsey KM, Yoshino J, Brace CS, Abrassart D, Kobayashi Y, Marcheva B, Hong HK, Chong JL, Buhr ED, Lee C, Takahashi JS, Imai S, Bass J (2009) Circadian clock feedback cycle through NAMPT-mediated NAD+ biosynthesis. Science 324:651–654.
Revollo JR, Grimm AA, Imai S (2004) The NAD biosynthesis pathway mediated by nicotinamide phosphoribosyltransferase regulates Sir2 activity in mammalian cells. J Biol Chem 279:50754–50763.
Rogina B, Helfand SL (2004) Sir2 mediates longevity in the fly through a pathway related to calorie restriction. Proc Natl Acad Sci U S A 101:15998–16003.
Sagar SM, Sharp FR, Curran T (1988) Expression of c-fos protein in brain: metabolic mapping at the cellular level. Science 240:1328–1331.
Sakurai T, Amemiya A, Ishii M, Matsuzaki I, Chemelli RM, Tanaka H, Williams SC, Richardson JA, Kozlowski GP, Wilson S, Arch JR, Buckingham RE, Haynes AC, Carr SA, Annan RS, McNulty DE, Liu WS, Terrett JA, Elshourbagy NA, Bergsma DJ, Yanagisawa M (1998) Orexins and orexin receptors: a

family of hypothalamic neuropeptides and G protein-coupled receptors that regulate feeding behavior. Cell 92:573–585.

Schwer B, Verdin E (2008) Conserved metabolic regulatory functions of sirtuins. Cell Metab 7:104–112.

Sinclair DA (2005) Toward a unified theory of caloric restriction and longevity regulation. Mech Ageing Dev 126:987–1002.

Stephan FK (2002) The "other" circadian system: food as a zeitgeber. J Biol Rhythms 17:284–292.

Tissenbaum HA, Guarente L (2001) Increased dosage of a *sir-2* gene extends lifespan in *Caenorhabditis elegans.* Nature 410:227–230.

Vallone D, Pignatelli M, Grammatikopoulos G, Ruocco L, Bozzi Y, Westphal H, Borrelli E, Sadile AG (2002) Activity, non-selective attention and emotionality in dopamine D2/D3 receptor knock-out mice. Behav Brain Res 130:141–148.

Wang J, Xu G, Slunt HH, Gonzales V, Coonfield M, Fromholt D, Copeland NG, Jenkins NA, Borchelt DR (2005) Coincident thresholds of mutant protein for paralytic disease and protein aggregation caused by restrictively expressed superoxide dismutase cDNA. Neurobiol Dis 20:943–952.

Wang T, Hung CC, Randall DJ (2006) The comparative physiology of food deprivation: from feast to famine. Annu Rev Physiol 68:223–251.

Wang Y, Tissenbaum HA (2006) Overlapping and distinct functions for a *Caenorhabditis elegans* SIR2 and DAF-16/FOXO. Mech Ageing Dev 127:48–56.

Weindruch R, Walford RL (1982) Dietary restriction in mice beginning at 1 year of age: effect on life-span and spontaneous cancer incidence. Science 215:1415–1418.

Weindruch R, Walford RL, Fligiel S, Guthrie D (1986) The retardation of aging in mice by dietary restriction: longevity, cancer, immunity, and lifetime energy intake. J Nutrit 116:641–654.

Wozniak DF, Hartman RE, Boyle MP, Vogt SK, Brooks AR, Tenkova T, Young C, Olney JW, Muglia LJ (2004) Apoptotic neurodegeneration induced by ethanol in neonatal mice is associated with profound learning/memory deficits in juveniles followed by progressive functional recovery in adults. Neurobiol Dis 17:403–414.

Yamanaka A, Beuckmann CT, Willie JT, Hara J, Tsujino N, Mieda M, Tominaga M, Yagami K, Sugiyama F, Goto K, Yanagisawa M, Sakurai T (2003) Hypothalamic orexin neurons regulate arousal according to energy balance in mice. Neuron 38:701–713.

Yu BP, Masoro EJ, McMahan CA (1985) Nutritional influences on aging of Fischer 344 rats: I. Physical, metabolic, and longevity characteristics. J Gerontol 40:657–670.